Heliyon 10 (2024) e37076

Contents lists available at ScienceDirect

Heliyon

journal homepage: www.cell.com/heliyon

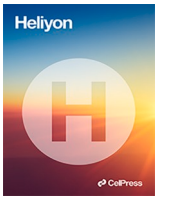

Research article

Eight types of RNA modification regulators define clinical outcome and immune response in gastric cancer

Danhong Dong [1], Pengfei Yu [1], Xin Guo [1], Jinqiang Liu, Xisheng Yang, Gang Ji, Xiaohua Li, Jiangpeng Wei [*]

Department of Digestive Surgery, Xijing Hospital, Air Force Military Medical University, Xi'an, Shaanxi, China

A R T I C L E I N F O

Keywords:
RNA modification
Gastric cancer
Tumor microenvironment
Prognosis
Immunotherapy

A B S T R A C T

Background: RNA modifications represent a novel category of biological molecule alterations, characterized by three primary classes of proteins: writers, erasers, and readers. Numerous studies indicate that the dysregulation of these RNA modifications is linked to cancer development and may offer new therapeutic avenues for treatment. In our research, we focused on eight specific genes associated with RNA modifications (RMRGs) to comprehensively analyze their distinct functions in gastric cancer (GC). Furthermore, we aimed to elucidate the roles of RMRGs concerning clinicopathological characteristics, tumor microenvironment, and patient prognosis.

Methods: In this study, we examined the expression and mutations of RMRGs in gastric cancer (GC) using data from TCGA-STAD (The Cancer Genome Atlas; Stomach adenocarcinoma) and the gene expression omnibus (GSE66229). We identified two subtypes of RMRGs and three gene clusters through consensus clustering analysis, assessing their differences in prognosis and immune cell infiltration patterns. Subsequently, we developed an RMRGs score to evaluate GC prognosis and highlight general immune features within the tumor microenvironment (TME). Lastly, we focused on MAMDC2 to validate its expression in GC and explore the effects of a MAMDC2 inhibitor on GC tumor cells.

Results: We discovered 94 differentially expressed RMRGs common to both the TCGA-STAD and GEO datasets. Notable differences in prognosis and immune cell infiltration were observed between the two RMRGs subtypes and three gene clusters. The RMRGs score emerged as an independent prognostic factor related to the tumor microenvironment (TME) characteristics in gastric cancer (GC). Reducing MAMDC2 levels enhanced cell migration and invasion while decreasing proliferation in vitro.

Conclusions: In conclusion, this study comprehensively analyzed the role of RMRGs on GC. Our study firstly proposed RMRGs score and demonstrated its potential to be biomarkers for prognosis and immune characteristics. Consequently, RMRGs score is of great clinical significance and can be utilized to develop individualized.

* Corresponding author.
E-mail address: weijiangpeng2015@163.com (J. Wei).
[1] These authors contributed equally to this paper as first author.

https://doi.org/10.1016/j.heliyon.2024.e37076
Received 27 May 2024; Received in revised form 26 August 2024; Accepted 27 August 2024
Available online 4 September 2024

1. Introduction

Gastric cancer (GC) is a leading cause of cancer-related deaths worldwide, accounting for 762,300 fatalities in 2022. The incidence and mortality rates of GC vary significantly by region, with higher prevalence observed in Asia, Africa, South America, and Eastern Europe [1]. Key risk factors for GC include *H. pylori* infection, certain lifestyle choices (such as smoking and diets rich in nitrates and nitrites), and genetic predispositions [2]. Treatment options for patients with GC encompass chemotherapy, radiotherapy, surgical intervention, targeted therapies, and immunotherapy. Numerous studies have shown that immunotherapy has achieved significant advancements in both research and clinical settings [3,4]. Despite the treatment's implementation, it has shown a highly variable objective response rate [5] and only modestly enhanced outcomes for patients with GC [6]. This variability is attributed to significant inter-patient and intra-patient genomic heterogeneity. Driven by the necessity for personalized therapy, classifying GC patients through innovative genomic research represents a key challenge for the future.

RNA modification represents a novel type of biological molecule alteration and consists of three distinct classes of proteins: writers, erasers, and readers. A substantial body of evidence indicates that the dysregulation of RNA modifications plays a role in cancer development and may offer potential therapeutic avenues [7]. This study concentrates on eight specific RNA modifications most closely linked to cancer pathogenesis. Among these, N6-methyladenosine (m6A) methylation, which involves the addition of a methyl group to adenosine at the sixth position, is the most prominent RNA modification. Elevated levels of m6A have been observed in gastric cancer (GC) and are correlated with poor prognosis [8]. The decrease of m6A levels has been shown to accelerate the progression of GC by activating the oncogenic WNT/PI3K-AKT signaling pathway and enhancing malignant characteristics in GC cells [9]. N1-Methyladenosine (m1A) methylation primarily occurs in transfer RNA (tRNA). The enzyme ALKBH3 removes m1A from tRNA, thereby facilitating cancer development [10]. Additionally,the TRMT6/TRMT61A complex enhances m1A methylation in tRNA and contributes to liver tumorigenesis through its activation.

Cholesterol synthesis and the self-renewal capacity of liver cancer stem cells are influenced by RNA modifications, which have shown significant therapeutic effects against liver cancer [11]. One such modification is 5-methylcytosine (m5C), which occurs at position 5 of cytidine residues. Research has demonstrated that m5C is linked to several types of cancer, including pancreatic cancer, bladder cancer, and GC [12–14]. In GC, NSUN2 serves as a predictor of poor outcomes and enhances cell proliferation, invasion, and migration [14]. m7G methylation promotes oncogenic transformation by affecting the metabolism of various RNA species, including mRNA, rRNA, miRNA, and tRNA [15–18]. While uridine-to-pseudouridine (Ψ) modifications typically function as tumor suppressors, their mechanisms and effects in cancer require further investigation [19–21]. Conversely, enzymes related to 5-methoxycarbonylmethyl-2-thiouridine (mcm5s2U), such as CTU1 and CTU2, are often implicated in advancing tumor progression [22]. The specific roles of adenosine-to-inosine editing (A-to-I) vary significantly depending on the type of cancer [7]. Overall, these findings indicate that these eight RNA modifications play crucial roles in influencing cancer progression and predicting patient prognosis. However, existing research has primarily concentrated on individual RNA modifications, leaving the interactions among different regulators unclear.

In the present study, we attempted to gain a comprehensive understanding of the role of eight kinds of RNA modification in GC development as well as its potential for GC immune treatment. Thus, we explored the expression patterns of RNA modification-related genes (RMRGs) and quantified RMRGs subtypes based on these RNRGs expression. We assessed the crosstalk between RMRGs subtypes and immune microenvironment, responsiveness to immunotherapy. In addition, we developed a novel nomogram model for GC prognostic prediction based on RMRGs score. We firstly presented the use of RMRGs scores to quantify the RMRGs subtype of each GC patient, thereby effectively predicting patient outcome and developing personalized immunotherapy strategies for GC patients.

2. Methods

2.1. Data download and processing

From the GDC (https://portal.gdc.cancer.gov/cart) downloaded the Cancer Genome Atlas (TCGA)-STAD datasets, including gene expression spectrum, somatic mutation data, and clinical information. The microarray datasets of STAD patients with clinical data were obtained from the gene expression omnibus (GEO) (https://www.ncbi.nlm.nih.gov/geo/). The study included two GEO-STAD datasets (GSE66229 and GSE84437), of which GSE66229 contains 100 STAD tumors and 300 normal tissues (GSE62254), and GSE84437 contains 433 tumor samples. The microarray datasets GSE66229 and TCGA-STAD datasets were analyzed for differential expression of RNA modification-related genes. Log2 transformation, and then used quantile normalization to process microarray data.

2.2. RNA modification-related gene expression

We identified RNA modification-related genes (RMRGs) associated with eight types of RNA modifications, namely m6A, m1A, m5C, Nm, m7G, Ψ, A-to-I, and mcm5s2U, through a review of recent literature [7]. Our study included a total of 140 RMRGs, which are detailed in Table S1. The expression differences of these RMRGs between normal tissues and tumors were analyzed using the R package limma and the Wilcox test. Differentially expressed RMRGs (DE-RMRGs) with P-values less than 0.05 were extracted from TCGA-STAD and GSE66229 datasets. Only those genes that appeared in both datasets were considered for further analysis.

2.3. Consensus clustering analysis of RMRGs

The gene expression data from TCGA-STAD were transformed into Transcript per Million (TPMs) format and combined with

datasets GSE84437 and GSE62254. This resulted in a total of 1108 STAD samples for further analysis. Using the expression profiles of DE-RMRGs in the merged datasets, we applied the consensus clustering method via the 'ConsensusCluster-Plus' package in R software to estimate unsupervised classes of STAD samples, yielding two distinct RNA modification patterns. To assess the clinical relevance of these patterns, we examined their associations with various clinicopathological features. Additionally, Kaplan-Meier survival analysis

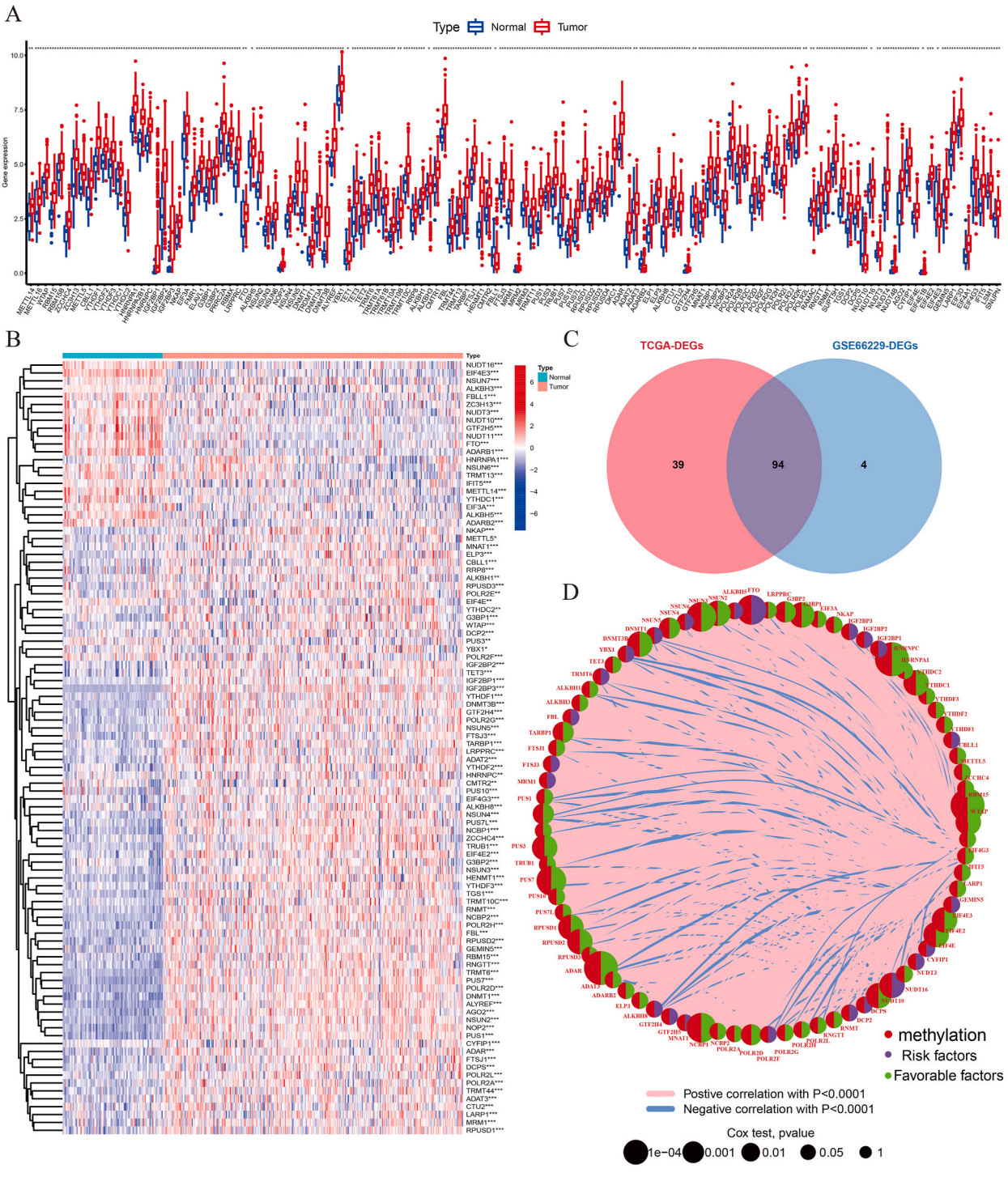

Fig. 1. RNA modification-related gene expression and prognosis analysis. The differential expression of RMRGs between normal and GC tissues in the TCGA-STAD(A) and GSE6629(B). (C) Venn of 94 overlapped DE-RMRGs between TCGA-STAD and GSE6629 dataset. (D) Network of DE-RMRGs interactions, regulatory relationships, and survival significance in GC.

was conducted to evaluate overall survival (OS) differences among STAD patients across the identified patterns. The single-sample gene-set enrichment analysis (ssGSEA) technique was utilized to determine the levels of infiltrating immune cells in STAD patients exhibiting different patterns. Furthermore, Gene Set Variation Analysis (GSVA) was performed using "c2. cp.kegg.v2022.1. Hs.symbols" from the MSigDB database to explore variations in biological functions between the two patterns.

2.4. Construction RMRGs score

To quantify the RMRGs subgroup of individual STAD patient, we constructed the RMRGs score. Firstly, the limma R package was employed to identify the differentially expressed genes (DEGs) in two RNA modification patterns with threshold of adjusted P value $<$ 0.05 and $|\log2(\text{fold change})| \geq 1$. Then, based on the expression of DEGs, 1108 STAD samples were divided into three gene clusters using "ConsensusClusterPlus" R package. Subsequently, differentially expressed genes (DEGs) that were positively and negatively correlated with the gene cluster signatures were categorized into RMRGs subgroup gene signatures A and B. To reduce the dimensionality of these subgroup gene signatures, we employed the Boruta algorithm, followed by principal component analysis to designate principal component 1 as the signature score. Finally, the RMRGs score of each STAD patient was calculated by the formula RMRGs score = $\sum$PC1A - $\sum$PC1B.

2.5. Prognosis analysis of RMRGs score

The STAD samples were classified into high-score and low-score groups according to the optimal cut-off value. The differences in OS time were recognized by survival and survminer R packages. The receiver operating characteristic curve (ROC) was showed the accuracy of the RMRGs score. The RMRGs score, age, gender, T stage and N stage were used to constructed univariate and multivariate Cox proportional hazards regression to determine whether RMRGs score was an independent predictor of prognosis. Furthermore, a nomogram, correction curves, ROC, and decision curve analysis (DCA)for the 1-, 3-, and 5-year OS were performed to access the predictive accuracy.

2.6. Tumor microenvironment and immunotherapy analysis of RMRGs score

The tumor microenvironment (TME) consists stromal cells and immune cells, therefore, the immune and stromal scores of each STAD patient was calculated by the ESTIMATE algorithm, and the difference in high and low-RMRGs score were showed by R package "ggpubr". Furthermore, the CIBERSORT algorithm was used to recognize the immune infiltration statuses in STAD patients. The difference between the RMRGs score and immune infiltration fraction was analyzed with the limma R package. Some immune checkpoint (IC) genes (Table S2) were utilized to detect if the high and low-RMRGs score had a distinct response to the immunotherapy. Tumor mutation burden (TMB) as an immunotherapy biomarker was associated with IC inhibitors responsiveness. The correlation between RMRGs score and TMB was explored. Also, somatic mutations data downloaded from TCGA were analyzed and visualized by maftools R package.

2.7. Gene enrichment analysis

Differentially expressed genes (DEGs) between high and low RMRG scores were identified using the "limma" R package, with results presented in a heatmap. To investigate gene functions and enriched pathways, Gene Ontology (GO) terms and KEGG enrichment analyses were carried out utilizing the clusterProfiler R package. Notably, since KEGG analysis focused solely on DEGs, some biologically significant genes that did not show marked differential expression might have been overlooked. Consequently, we applied the gene set enrichment analysis (GSEA) algorithm to include all genes in our evaluation.

2.8. Human gastric specimens

Tissue samples from human gastric tumors and adjacent non-tumor tissues (at least 5 cm away from the tumor) were obtained from 14 patients with comprehensive clinicopathological data at The First Affiliated Hospital of Air Force Military Medical University. All subjects underwent radical gastrectomy in 2022, and none had received preoperative chemotherapy or radiotherapy. Fresh specimens were immediately frozen in liquid nitrogen after resection for subsequent protein or RNA extraction. The study was approved by the Ethics Committee of The First Affiliated Hospital of Air Force Military Medical University (KY20212226-C-1), and informed written consent was secured from each patient prior to their participation.

2.9. Verification the expression of MAMDC2

The mRNA expression of MAMDC2 was evaluated by RT-qPCR. TRIzol reagent was used to isolated the total RNA from gastric tissues according to instructions of the manufacturer. The cDNA was transcripted by Evo M-MLV Kit (AG11706). The sequences of the qPCR primers are shown in Table S3. The real-time PCR was performed on SYBR Green Pro Taq HS kit (AG11701). The relative expression quality was calculated by the 2-ΔΔCt. The level of MAMDC2 protein was investigated by Western blot and immunohistochemical (IHC). The operation was performed according to the previous study [23].

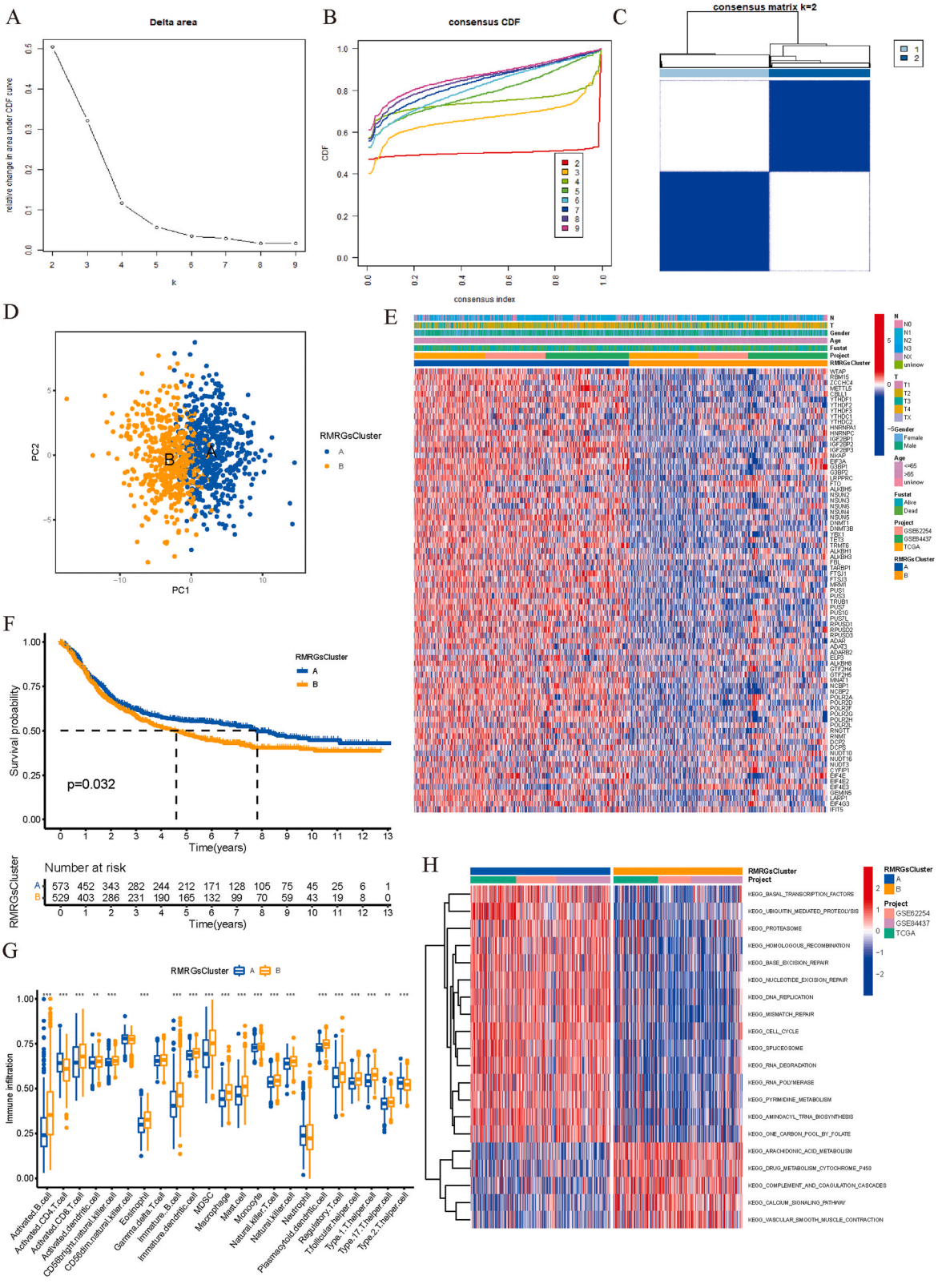

(caption on next page)

Fig. 2. Identification of RMRGs subtype in gastric cancer. (A) The CDF from k value = 2 to 9. (B) Relative variation of the area under the CDF region at k value = 2–9. (C) Consensus matrix at optimal k value = 2. (D) PCA of RMRGs expression profiles from the GC samples confirmed the two clusters. (E) Heatmap of clinical characteristics and RMRGs expressions among the two clusters. (F) Kaplan-Meier curves of OS time of RMRGs cluster A and cluster B. (G) The difference of immune cell infiltration between RMRGs cluster A and cluster B (*$P < 0.05$, **$P < 0.01$; ***$P < 0.001$). (H) GSVA enrichment analysis showed the activation status of biological behaviors in RMRGs clusters A and B.

2.10. SiRNA transfection

The siRNA sequences targeting MAMDC2 was shown in Supplementary Table 1 siRNA was transfection into SGC7901 and HGC27 tumor cell using Lipofectamine 3000 (Invitrogen), and RT-qPCR evaluate the inhibition efficiency of siRNA.

2.11. Wound healing assay

Cells were seeded into a 6-well plate at 3×10^5 cells/well and cultured until 100 % confluence. Using a 10 μl tip to scratch a line,

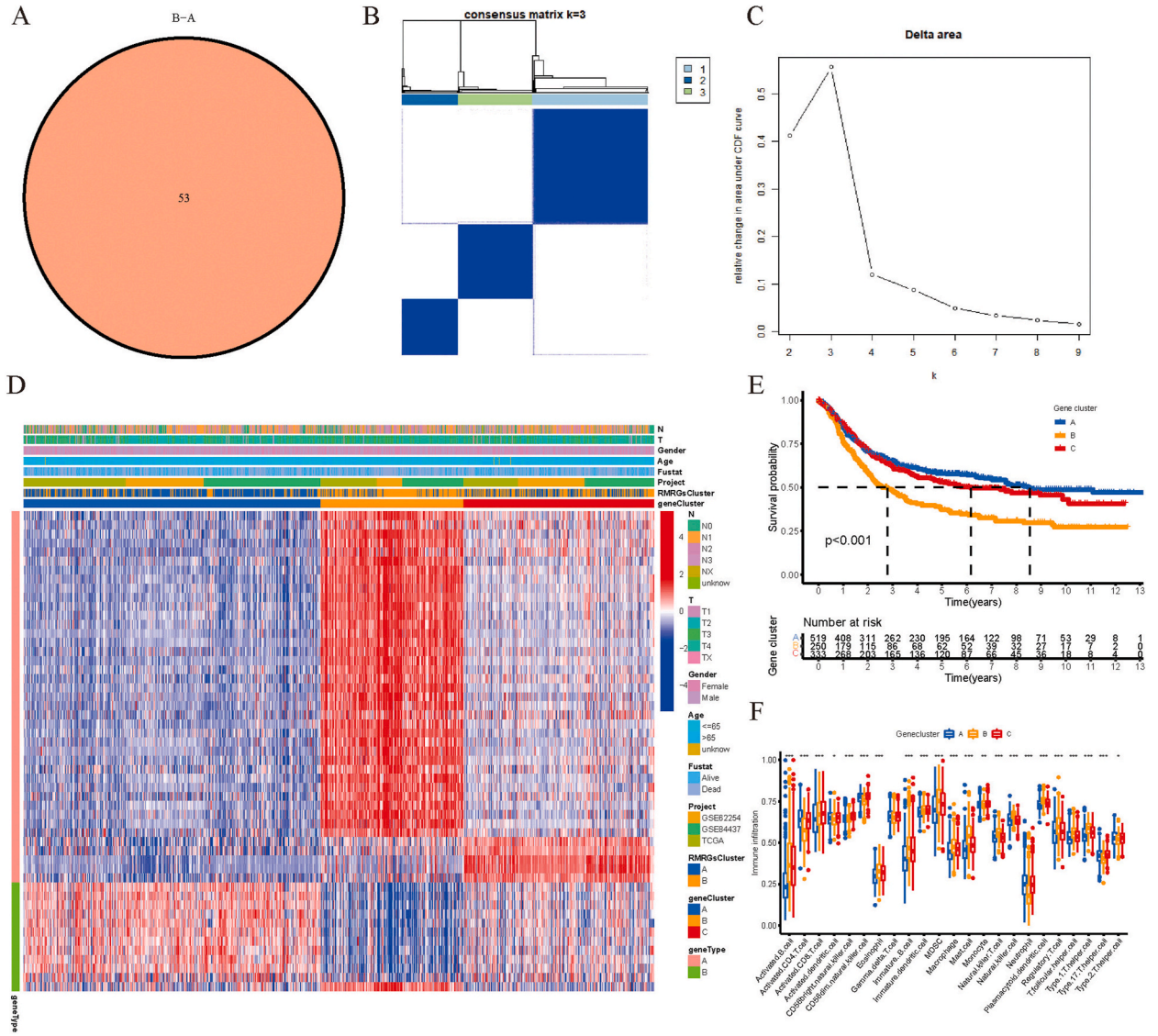

Fig. 3. Identification three RMRGs gene clusters for GC. (A) 53 DEGs between RMRGs cluster A and B. (3B, C) All samples were clustered into three gene clusters. (D) Clinical features of the three RMRGs gene clusters. (E) Kaplan-Meier survival analysis for GC patients in the three RMRGs gene clusters. (F) Boxplots showed the different abundance of 23 infiltrating immune cell types in three gene clusters (*$P < 0.05$, **$P < 0.01$; ***$P < 0.001$).

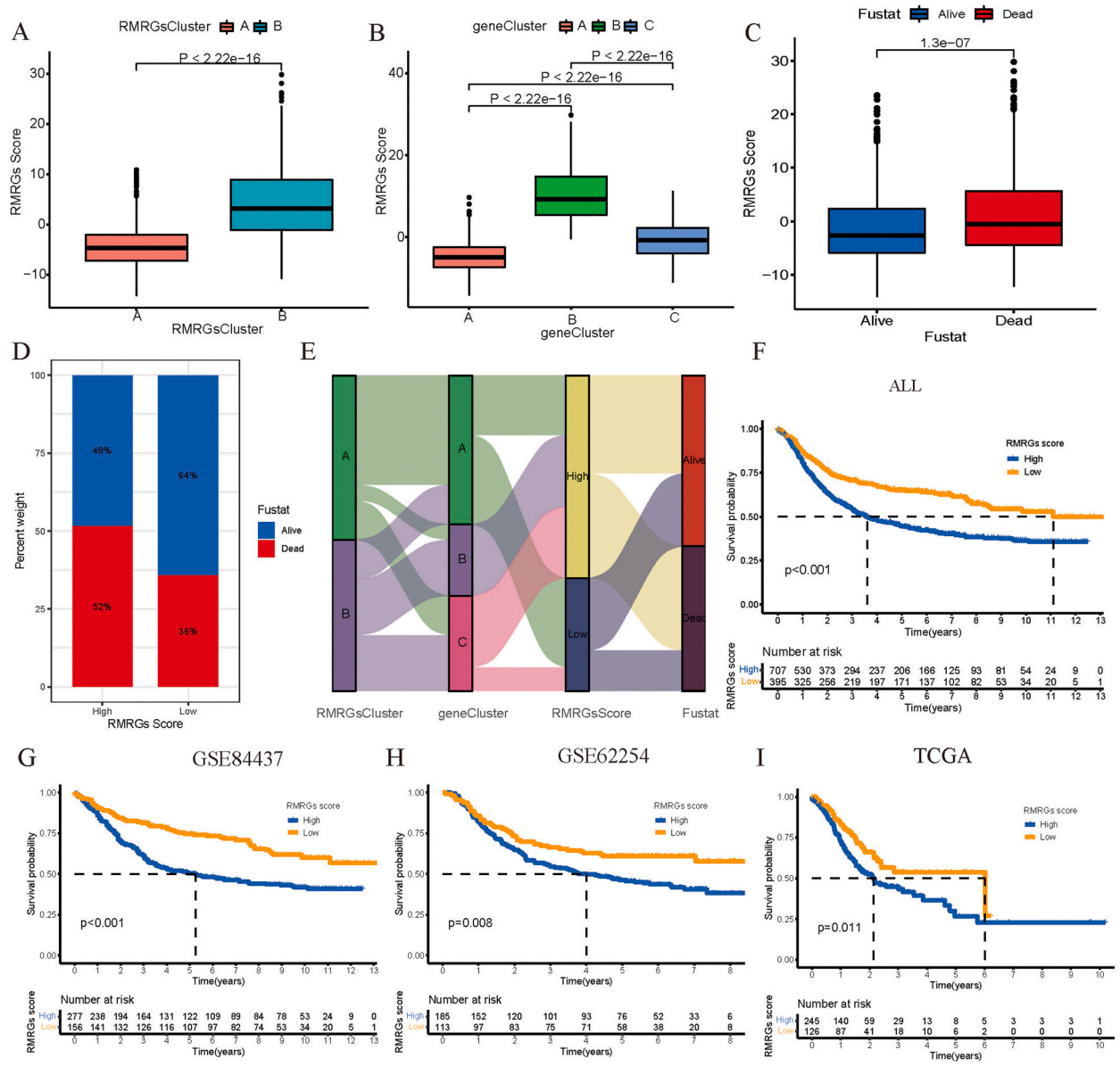

Fig. 4. Discrepancy in RMRGs score between the two RMRGs subtypes (A) and the three gene clusters (B). (C, D) Histogram and boxplot depicted the distribution of survival status of GC patients in the two scores. (E) Alluvial diagram of two RMRGs clusters, three gene clusters, RMRGs scores, and clinical outcomes. Kaplan-Meier analysis of the OS between the two RMRGs score in merged data (F), GSE84437 (G), GSE62254 (H), and TCGA (I).

and then cell debris were washed and cells were cultured in RPMI 1640 culture medium with 1 % FBS. The wound edges were measured at 0, 24, and 48 h, respectively.

2.12. Transwell assay

Cells (1×10^5) were seed the upper chamber and cultured at 37 °C, 5 % CO_2 for 48 h. Then, the chambers were placed in 4 % paraformaldehyde for 30 min and stained with 1 % crystal violet for 1 h. Cells that migrated toward the outer chamber were counted in five representative (200 ×) fields per insert.

2.13. CCK-8

Cells were seeded into a 96-well plate at 3000 cells/well, and cultured at 37 °C, 5 % CO_2. The OD value were measured at 1, 2, 3, 4,

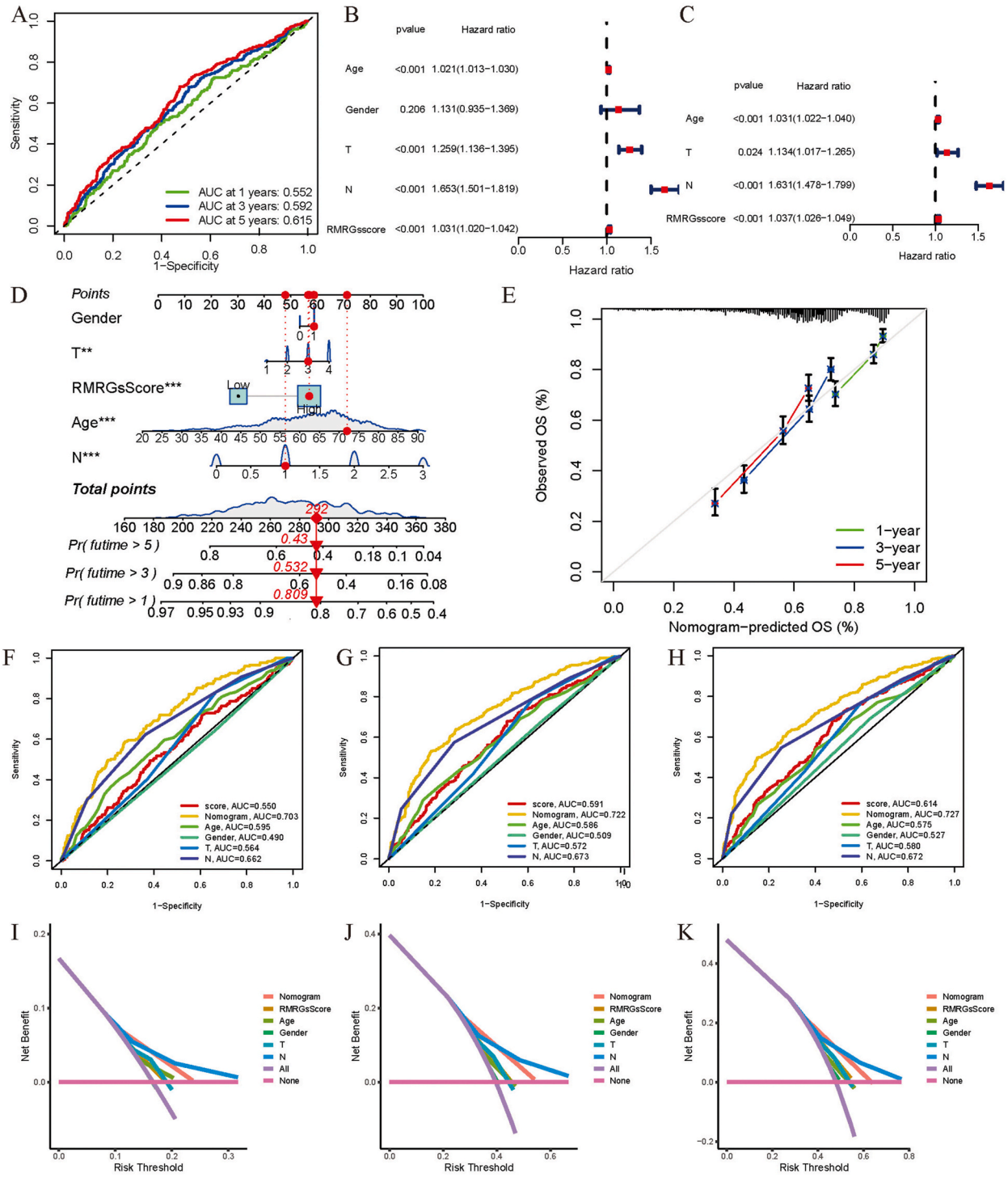

Fig. 5. Development of an independent prognostic model for GC based on RMRGs score. (A) Time-dependent ROC curve evaluated the predictive accuracy of RMRGs score for GC. The uniCox (B) and multiCox (C) analyses. (D) Constructing nomogram model for predicting the 1-, 3-, and 5-year OS. (E) Calibration curves for validating the established nomogram. (F–H) The ROC curves of the nomograms for predicting 1-, 3-, and 5-year OS in GC patients, respectively. (I–K) The DCA curves of the nomograms for predicting 1-, 3-, and 5-year OS in GC patients.

and 5 d.

2.14. Statistical analyses

The bioinformatics analyses were completed in R language (Version 4.1.2) and Perl (Version 5.30.0). And A P value of <0.05 was considered statistically significant.

3. Results

3.1. RNA modification-related gene expression

We attempted to determine the expression levels of 140 RMRGs in STAD tumor and normal tissues using TCGA-STAD and GSE6629 dataset. The expression level of 123 RMRGs had a significant difference between 32 normal and 375 STAD tumor tissues in TCGA-STAD dataset (Fig. 1A). Similarly, there are 98 DE-RMRGs in GSE6629 dataset (Fig. 1B). As shown in Figs. 1C and 94 overlapped

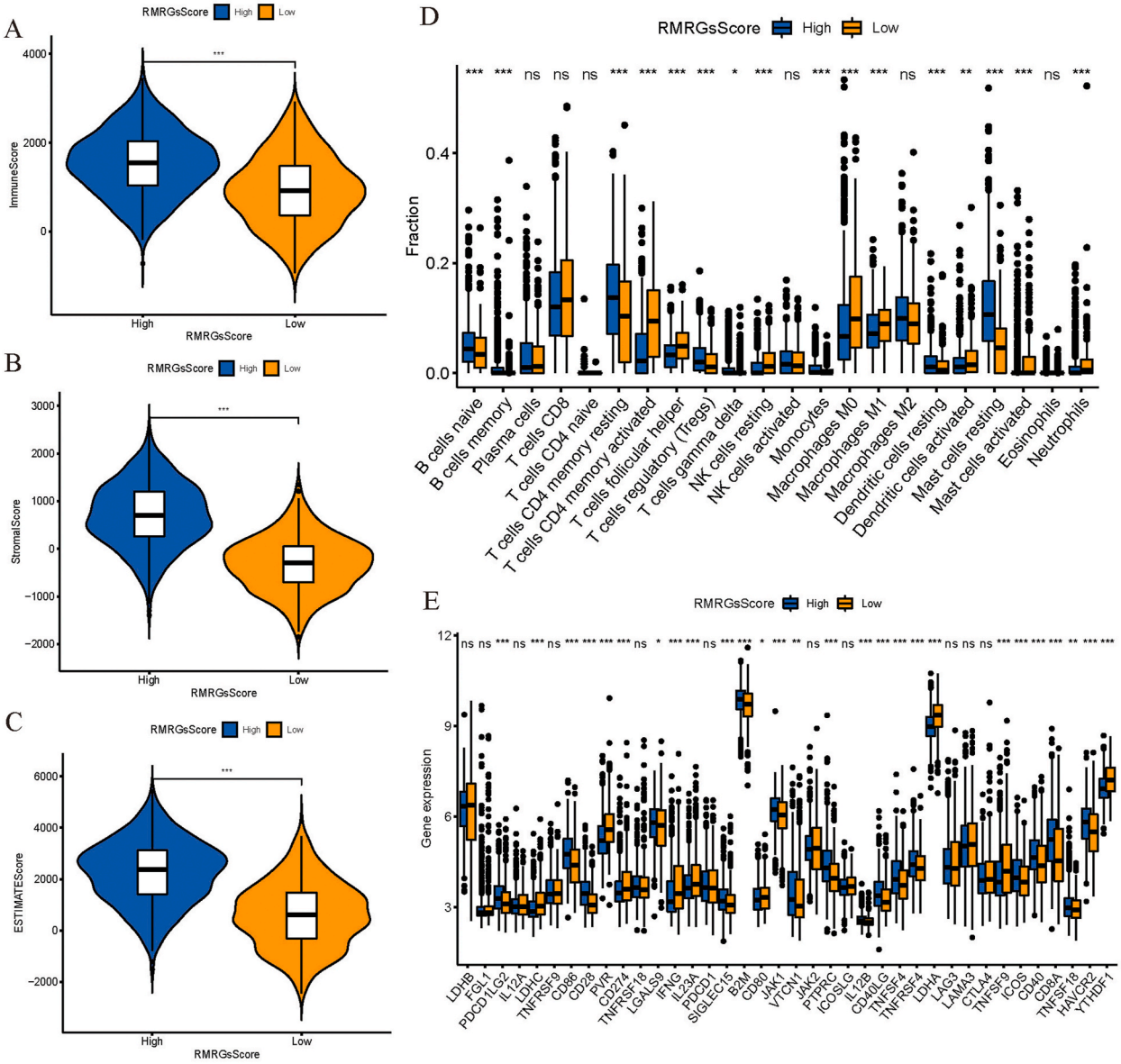

Fig. 6. Tumor microenvironment analysis of RMRGs Score. RMRGs score was related with ImmuneScores (A), StromalScore (B), and ESTIMATEScores(C). Boxplots show abundance of 23 infiltrating immune cell (D) and differences in ICs (E) for the two RMRGs score groups.

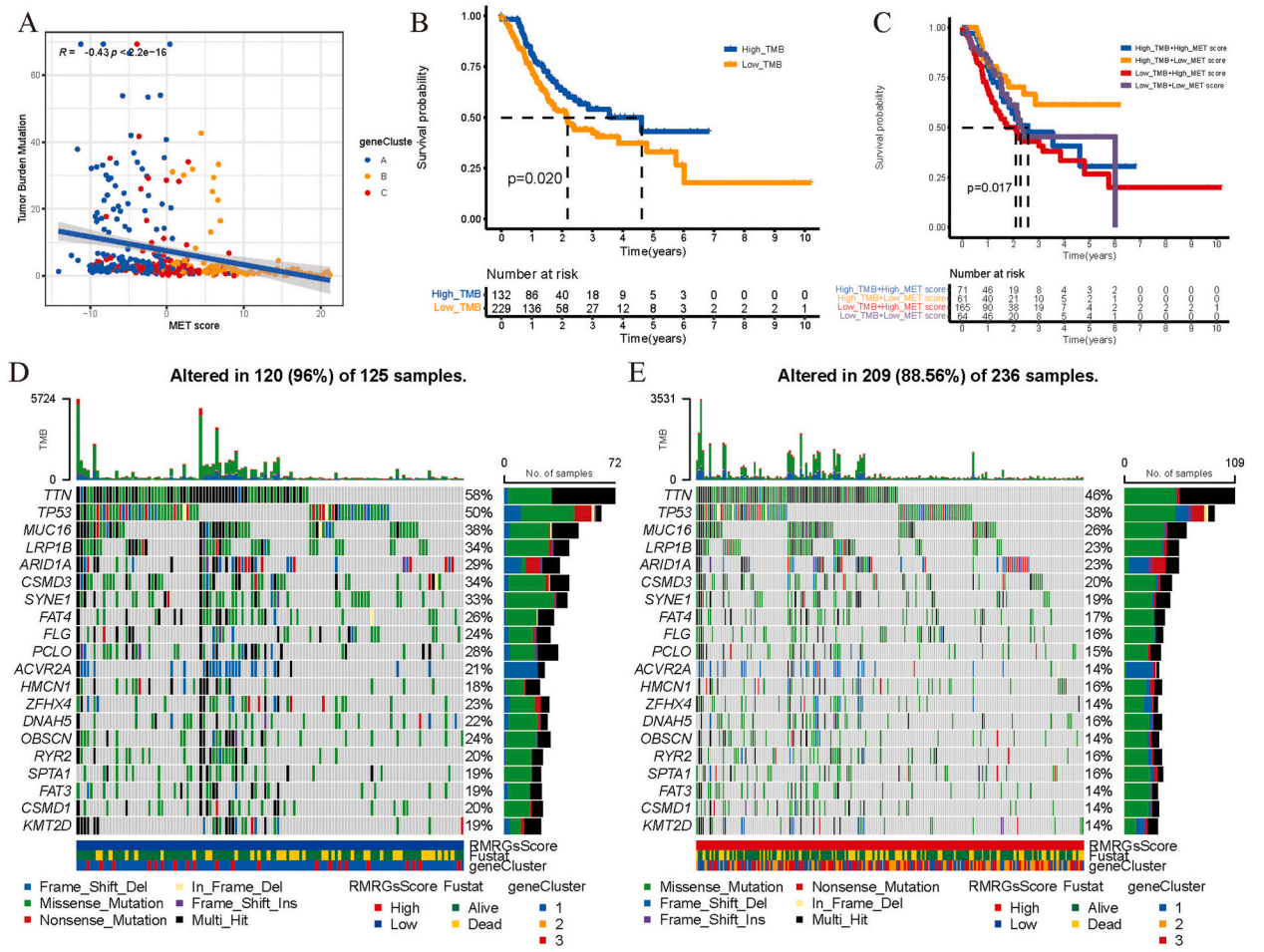

Fig. 7. RMRGs score is correlated with tumor mutation of GC. (A) RMRGs score was negatively correlated with TMB. (B) Kaplan-Meier analysis based on TMB. (C) Kaplan-Meier analysis combining TMB and the RMRGs score. Waterfall plot of mutation values in the low (D) and high (E) RMRGs score group.

DEGs were obtained (TableS4).

After merging TCGA-STAD, GSE62254 and GSE84437 datasets, we obtained the expression matrix of 14099 genes in 1108 gastric cancer sample. Of the 94 DE-RMRGs, we only extracted the expression levels of 79 genes from the merged dataset. Furthermore, we also analyzed the prognostic value of 79 DE-RMRGs for STAD patients by uniCox (TableS5), constructed the interaction network of DE-RMRGs, and evaluated its survival significance in gastric cancer patients (Fig. 1D).

3.2. Identification of RMRGs subtype in gastric cancer

Based on the expression level of 79 DE-RMRGs, consensus clustering method was employed to cluster the 1108 gastric cancer sample to further illustrate the biological differences among subgroups. The cumulative distribution function (CDF) curves indicated that when k = 2, the discrepancies between subgroups was minimal (Fig. 2A–D). Fig. 2E illustrates significant variations in the expression of RMRGs alongside clinical characteristics. As a result of Fig. 2F, the STAD patients of RMRGs cluster B showed poor survival compared with RMRGs cluster A. Additionally, there were more immune lymphocyte infiltration in RMRGs cluster B (Fig. 2G). The heatmap of GSVA showed the impact of RMRGs on TME enrichment, tumorigenesis, and tumor treatment-related pathways, such as The pathways involved include the arachidonic acid metabolic pathway and the calcium signaling pathway(Fig. 2H).

3.3. Identification three RMRGs gene clusters for gastric cancer

To further investigate the potential biological activity in two RMRGs subtype, 53 DEGs were screen out based on limma R package (Fig. 3A). GO enrichment analysis indicated that these DEGs were primarily associated with biological processes concerning chromosome segregation and nuclear division (Fig. 9A). KEGG enrichment showed cell cycle pathways are enriched (Fig. 9B). To further assess the RMRGs subtype, secondary clustering was conducted based on DEGs related to RMRGs, categorizing STAD patients into

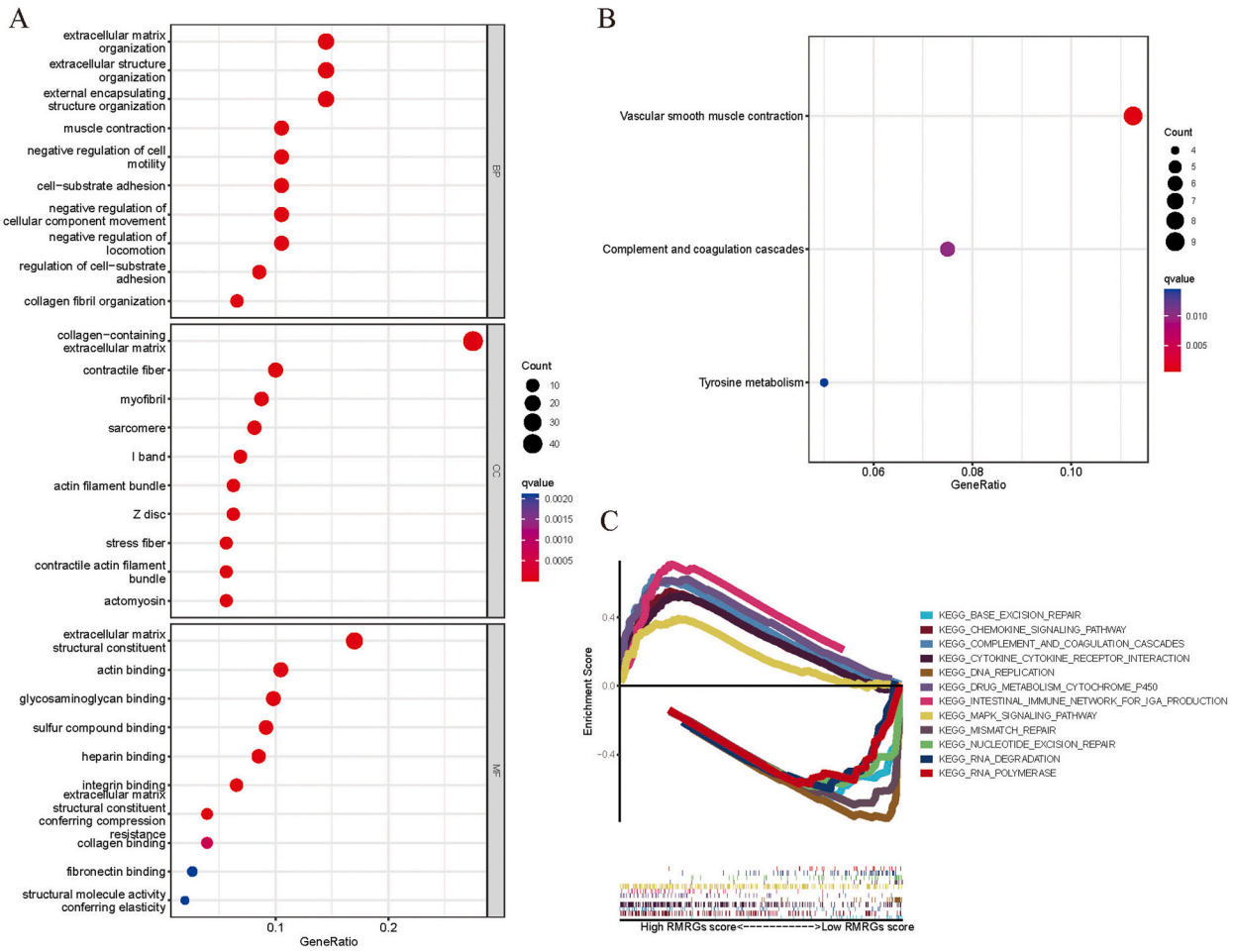

Fig. 8. Genes enrichment analysis. Go (A) and KEGG enrichment analysis (B) base on DEGs between high RMRGs score and low RMRGs score group. (C) GSEA analysis.

three distinct gene clusters associated with RMRGs phenotypes (Fig. 3B and C). GSVA results revealed that the majority of patients in gene cluster A were classified under RMRGs subtype A, whereas those in gene clusters B and C, which exhibited poorer prognoses, were categorized as RMRGs subtype B (Fig. 3D). Among these, STAD patients in gene cluster B displayed the least favorable prognosis along with increased immune lymphocyte infiltration (Fig. 3E and F).

3.4. Correlation RMRGs score with survival of GC patients

We determined that 52 RMRGs gene signature was related to gene cluster based on the Boruta algorithm. The RMRGs-A gene signature, comprising 41 genes, was found to be positively correlated with one of the gene clusters, while an additional 11 genes were assigned to the RMRGs-B gene cluster (Table S5). A PCA analysis was utilized to calculate the RMRGs score, which was then used to classify all gastric cancer patients into high or low RMRGs score groups. The relationship between the RMRGs score and the two clustering types revealed significant disparities across different clusters. Notably, the median RMRGs score for both RMRGs subtype B and gene cluster B was substantially higher compared to other clusters (Fig. 4A and B). Histogram and boxplot analyses indicated that gastric cancer patients with elevated RMRGs scores exhibited significantly higher mortality rates than those with lower scores (Fig. 4C and D). An alluvial plot illustrated the distribution of RMRGs scores among the two RMRGs clusters, three gene clusters, and the survival status of gastric cancer patients (Fig. 4E). Patients with high RMRGs scores experienced poorer outcomes compared to those with low RMRGs scores (Fig. 4F–I).

3.5. Independent prognostic analysis of RMRGs score

We found that the RMRGs score correlated significantly with survival status and time of GC patients. Additionally, the result of ROC showed that RMRGs score had better OS prediction accuracy at 1, 3, 5 years (Fig. 5A). Both univariate and multivariate Cox regression

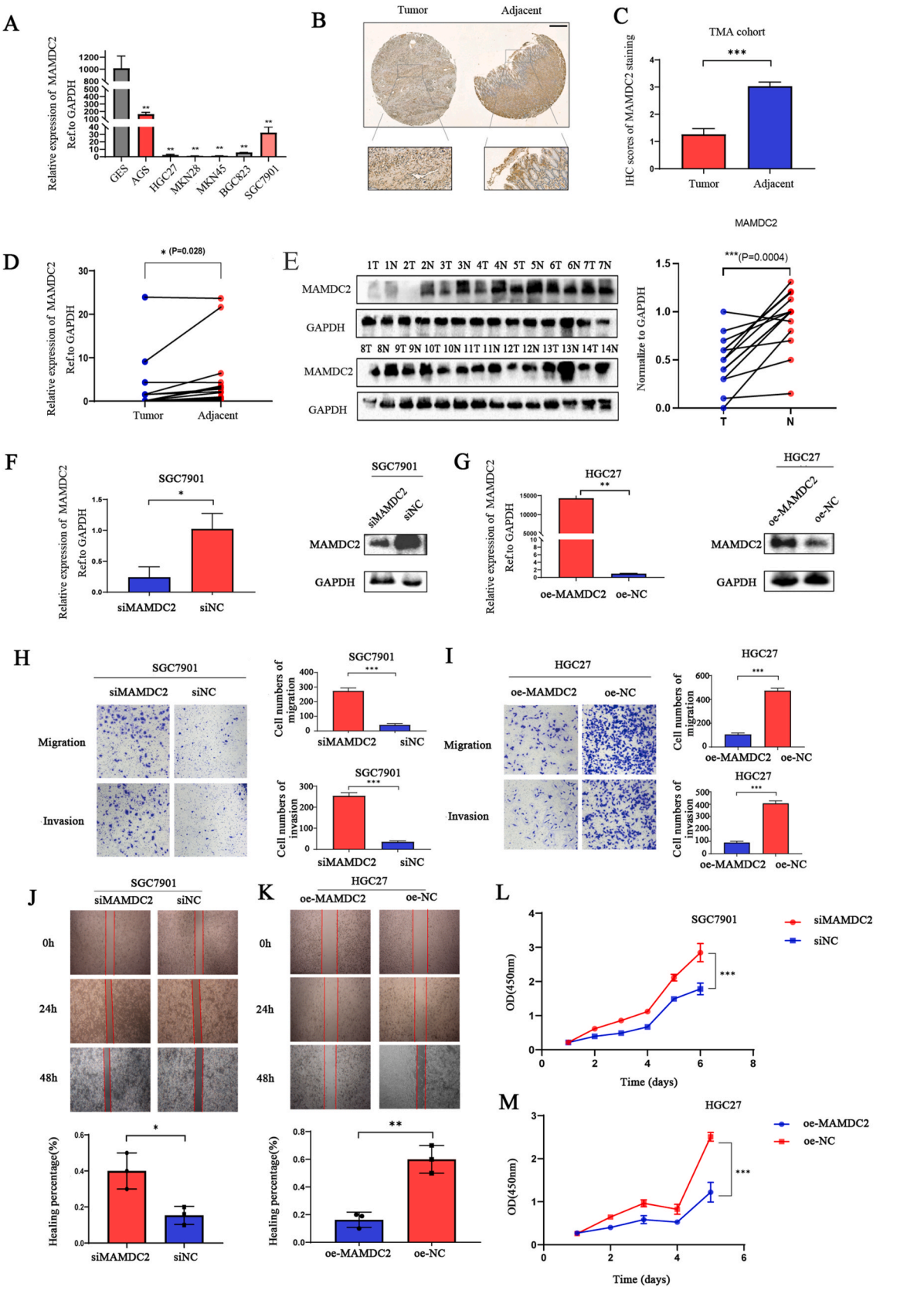

(caption on next page)

Fig. 9. Evaluation the impact of MAMDC2 on GC cell biologic behaviors. (A) The expression of MAMDC2 mRNA in GC cell; (B–E) Using IHC (B, C), RT-qPCR (D), and (E) Western blot investigated the expression of MAMDC2. (F, G) The siRNA significantly inhibited the expression of MAMDC in SGC7901 cell and HGC27 cell. (H–M) Depletion of MAMDC2 (Fig. 9H and I) increased the cell migration and invasion (Fig. 9J and K), promoted the wound healing (Fig. 9L and M), and impair the proliferation.

analyses indicated that the RMRGs score serves as an independent negative prognostic factor, demonstrating strong predictive capability (Fig. 5B and C). To intuitively calculate the OS time of GC patients at 1, 3, 5 years, we constructed a nomogram model incorporating the RMRGs score and other clinical factors to predict (Fig. 5D). The calibration curve of nomogram model elucidated that the observed values and predicted values were highly identical, that was, the nomogram model can effectively forecast the actual survival outcomes (Fig. 5E). The area under curve of ROC also showed that the nomogram had a satisfactory accuracy in predicting prognosis at 1, 3, 5 years (Fig. 5F–H). In addition, the nomogram had a better net benefit in forecasting the prognosis, as demonstrated in DCA curve (Fig. 5I–K).

3.6. Tumor microenvironment analysis of RMRGs score

Correlation analysis demonstrated that the RMRGs score was positively associated with immune score, stromal score, and ESTIMATE, signifying a different TME characterize in two groups (Fig. 6A,B,C). By quantifying the degree of immune lymphocyte cell infiltration in the GC samples, we observed that 8 immune cells were associated with the high-RMRGs score group, including Treg cell. However, the M0 and M1 macrophages cells and other 6 kinds of immune cell were associated with the low-RMRGs group (Fig. 6D). Furthermore, the relationship between immune checkpoints and RMRGs scores was assessed and 27 differentially expressed immune checkpoints were found(Fig. 6E).

3.7. RMRGs score is correlated with tumor mutation of GC

The RMRGs score exhibited a negative correlation with tumor mutation burden (TMB) (Fig. 7A). Additionally, gastric cancer patients with low TMB had poorer prognoses compared to those with high TMB levels (Fig. 7B). To evaluate the combined impact of TMB and RMRGs score on prognosis, both factors were analyzed together. Among the four groups examined, gastric cancer patients with high TMB and low RMRGs scores experienced the shortest survival time (Fig. 7C). Moreover, we also compared the distributional discrepancy of tumor somatic cell mutation characteristics between high and low RMRGs score group. The oncoplot illustrated the top 20 driver genes with the most frequent mutations. It was observed that mutations in these genes were more prevalent in patients with low RMRGs scores compared to those with high RMRGs scores (Fig. 7D and E).

3.8. Genes enrichment analysis

To investigate the variations in biological functions and pathways between groups with high and low RMRGs scores, we identified DEGs in both groups. These DEGs were then subjected to GO and KEGG enrichment analyses, along with GSEA. The result of GO showed in Fig. 8A. KEGG analysis showed that DEGs might play a role in some pathways such as vascular smooth muscle contraction, complement and coagulation cascades, and tyrosine metabolism (Fig. 8B). The GSEA findings revealed that the high RMRGs score group showed enrichment in pathways related to the intestinal immune network for IgA production, MAPK signaling, chemokine signaling, complement and coagulation cascades, as well as cytokine-cytokine receptor interactions. In contrast, the low RMRGs score group exhibited enrichment in several DNA and RNA damage repair pathways, including mismatch repair, RNA degradation, DNA replication, base excision repair, and nucleotide excision repair (Fig. 8C).

3.9. Evaluation the impact of MAMDC2 on GC cell biologic behaviors

We determined that 52 RMRGs gene signature was related to RMRGs score. Fig. 9A showed the significantly differential expression in GC ($P < 0.001$). MAMDC2 (meprin/A-5 protein/receptor protein-tyrosine phosphatase mu domain containing 2) was selected to validate the expression in GC tissues and cell. The relative mRNA level of MAMDC2 was downregulated in GC cells (Fig. 9A) and GC tumor tissues (Fig. 9D). Meanwhile, the MAMDC2 protein was also significantly downregulated in tumor tissues (Fig. 9 B, C, E). The siRNA sequences targeting MAMDC2 can significantly inhibit the expression of MAMDC2 in SGC7901 cell (Fig. 9F) and HGC27 (Fig. 9G). Depletion of MAMDC2 increased the SGC7901 cell migration and invasion (Fig. 9H), which was consistent with the result obtained from the HGC27 cell (Fig. 9I). Inhibiting the expression of MAMDC2 in SGC7901 cell and HGC27 cell can promote the wound healing (Fig. 9J and K), impair the proliferation (Fig. 9L and M).

4. Discussion

Recent advancements in genomics have revealed that RNA modifications are often dysregulated in human cancers, influencing tumor progression and potentially serving as a therapeutic approach. There exist more than 100 distinct post-synthetic modifications of RNA [7]. Moreover, accumulating evidence indicates that numerous enzymes involved in RNA modification play significant roles in GC progression and may serve as prospective treatment targets and prognostic biomarkers for GC [8,9,14]. Prior research has primarily

concentrated on the prognostic or therapeutic implications of individual RNA modification regulators in GC, often overlooking the interactions between different RNA modifications. In our study, we assessed a total of 140 RNA modification enzymes across eight modification types to classify subtypes of GC patients and examined differences in prognosis and tumor microenvironment (TME) among these subtypes.

In this investigation, we first discovered 79 differentially expressed RNA modification-related genes (DE-RMRGs) using data from the TCGA-STAD, GSE62254, and GSE84437 datasets. Utilizing the expression profiles of these DE-RMRGs, we classified them into two distinct RMRG clusters. The results indicated significant differences in patient outcomes and immune cell infiltration characteristics between the clusters, with cluster-B of RMRGs showing a worse prognosis and heightened levels of immune cell infiltration. Following this, we discovered three gene clusters associated with RMRGs, which also demonstrated significant differences in patient prognosis and immune cell infiltration. These findings suggest a potential regulatory relationship between RMRGs and gastric cancer (GC). It is important to note that GC is a complex and highly heterogeneous condition [24]. Creating a molecular subtype for gastric cancer (GC) to inform clinical treatment strategies presents a significant challenge for the future [25]. To address this, we aimed to develop an RMRGs scoring model using PCA analysis to stratify patients with GC. Our results demonstrated that patients with elevated RMRGs scores experienced worse outcomes in comparison to those with lower scores, a finding corroborated by data from the TCGA, GSE84437, and GSE66254 datasets. Furthermore, univariate and multivariate Cox regression analyses indicated that the RMRGs score is linked to a higher risk of poor prognosis. To enhance the accuracy of outcome predictions, we devised a quantified nomogram prognostic model that incorporates RMRGs scores along with other clinical parameters.

Immunotherapy is emerging as one of the most significant advancements in cancer treatment, particularly with immune checkpoint inhibitors (ICIs) showing remarkable success across various solid tumors, including gastric cancer (GC) [26]. By inhibiting the binding of immune checkpoint ligands to their receptors, immune checkpoint inhibitors (ICIs) can enhance the immune response targeting tumors. Programmed death ligand-1 (PD-L1), produced by the CD274 gene, is mainly found on antigen-presenting cells and various tumor cells. When PD-L1 binds to PD-1, it triggers immunosuppressive signaling pathways that suppress T-cell activity and facilitate tumor immune evasion [27]. PD-L1 inhibitors have employed the management of advanced GC, especially for late line treatments. However, only a subset of GC patients has the ideal objective response rate(ORR) and benefit from this ICIs therapy due to the heterogeneity of TME [28]. Therefore, it is crucial to identify biomarkers that can assess the clinical effectiveness of immune checkpoint inhibitors (ICIs). Several studies have demonstrated that PD-L1 expression plays a significant role in immunotherapy for gastric cancer (GC) [29]. The Combined Positive Score (CPS) serves as a method for evaluating PD-L1 levels in both tumor cells and associated immune cells in GC. Patients with a CPS of 10 or higher tend to benefit significantly from second-line treatment with pembrolizumab, showing improved clinical outcomes [30]. In this study, we found varying levels of PD-L1 expression between groups with low and high RMRGs scores. This variation was also noted in the expression levels of several immune checkpoints.

Tumor mutational burden (TMB) is recognized as a reliable biomarker for predicting response to immune checkpoint inhibitors (ICIs) across various cancers [5]. In the KEYNOTE-061 trial, patients with advanced gastric cancer (GC) exhibiting higher TMB demonstrated improved overall response rates (ORR) and extended overall survival (OS) [31]. Another investigation highlighted that patients with elevated TMB experienced significantly better clinical outcomes compared to those with lower TMB levels (ORR: 33.3 % vs. 7.1 %, OS: 14.6 months vs. 4.0 months) [32]. These findings suggest a positive correlation between TMB and clinical response to ICIs, leading to favorable prognoses. Consistent with this, our study also showed that patients with high TMB had better prognostic outcomes than those with low TMB. Additionally, we noted an inverse relationship between RMRGs scores and TMB, suggesting that a lower score might be associated with higher ORR from ICIs. Gene function enrichment analysis revealed that pathways related to mismatch repair, RNA degradation, DNA replication, base excision repair, and nucleotide excision repair were more prominent in the group with lower RMRGs scores.

Furthermore, we identified 52 gene signatures associated with RMRGs scores. Notably, the expression of MAMDC2 was significantly altered in gastric cancer. Its differential expression was confirmed through RT-qPCR, western blotting, and immunohistochemistry (IHC). MAMDC2 is a secretory protein composed of 686 amino acids, featuring a short N-terminal signal sequence along with four consecutive domains. This gene has been shown to be differentially regulated in various cancers, including chronic myeloid leukemia, head and neck squamous cell carcinoma, and breast cancer [33–35]. In breast cancer, downregulation of MAMDC2 has been linked to significant prognostic implications [36]. Similarly, lower levels of MAMDC2 were associated with survival outcomes in gastric cancer (GC). Overexpression of MAMDC2 led to increased cell death in T-47D cells (a breast cancer line) and reduced tumor cell proliferation in vivo [36]. Our findings indicated that depletion of MAMDC2 enhanced cell migration and invasion while inhibiting cell proliferation in vitro. The observed discrepancies may be attributed to the effects of the tumor microenvironment in vivo.

While our research is based on secondary analyses of data from public databases, it does have certain limitations. The retrospective nature of these datasets introduces potential selection bias, which may impact the reliability of the findings. Therefore, additional prospective studies are necessary to validate our conclusions.

5. Conclusion

In conclusion, we conducted an in-depth analysis of the impact of RMRGs on GC and elucidated their significance regarding clinicopathological characteristics, TME, and patient prognosis. Additionally, we established an RMRGs score and highlighted its potential as a biomarker for predicting outcomes and responses to immunotherapy. As a result, the RMRGs score holds substantial clinical relevance and can aid in formulating personalized immunotherapeutic approaches for patients with GC.

Ethical statement

All research was approved by the Ethics Committee of the First Affiliated Hospital of Air Force Military Medical University (KY20212226-C-1). Informed written consent was obtained from each of the patients before enrollment.

Data availability statement

All data come from the publicly available datasets in present study. These datasets can be found here: TCGA database (http://cancergenome.nih.gov/), the GEO database (GSE66229) (GSE62254) (GSE84437) were included in this study, MSigDB datasets (http://www.gsea-msigdb.org/gsea/msigdb/index.jsp).

CRediT authorship contribution statement

Danhong Dong: Writing – original draft, Validation, Resources, Project administration, Methodology, Investigation, Conceptualization. **Pengfei Yu:** Writing – review & editing, Validation, Resources, Investigation, Formal analysis, Data curation, Conceptualization. **Xin Guo:** Writing – review & editing, Supervision, Software, Project administration, Methodology, Formal analysis, Data curation, Conceptualization. **Jinqiang Liu:** Writing – review & editing, Visualization, Software, Project administration, Investigation, Conceptualization. **Xisheng Yang:** Writing – review & editing, Software, Resources, Methodology, Investigation, Funding acquisition, Conceptualization. **Gang Ji:** Writing – review & editing, Validation, Software, Resources, Investigation, Formal analysis, Data curation, Conceptualization. **Xiaohua Li:** Writing – review & editing, Validation, Supervision, Resources, Funding acquisition, Data curation. **Jiangpeng Wei:** Writing – original draft, Supervision, Software, Project administration, Methodology, Investigation, Funding acquisition, Formal analysis.

Declaration of competing interest

All authors have made outstanding contributions to the study; all authors have reviewed the manuscript and have consented to its submission; all authors declare no conflicts of interest. Neither the entire paper nor any part of it has been submitted or published elsewhere.

Appendix A. Supplementary data

Supplementary data to this article can be found online at https://doi.org/10.1016/j.heliyon.2024.e37076.

References

[1] H. Sung, J. Ferlay, R.L. Siegel, et al., Global cancer statistics 2020: GLOBOCAN estimates of incidence and mortality worldwide for 36 cancers in 185 countries, CA Cancer J Clin 71 (3) (2021) 209–249.
[2] E.C. Smyth, M. Nilsson, H.I. Grabsch, et al., Gastric cancer, Lancet 396 (10251) (2020) 635–648.
[3] K. Muro, H.C. Chung, V. Shankaran, et al., Pembrolizumab for patients with PD-L1-positive advanced gastric cancer (KEYNOTE-012): a multicentre, open-label, phase 1b trial, Lancet Oncol. 17 (6) (2016) 717–726.
[4] Y.Y. Janjigian, A. Kawazoe, P. Yanez, et al., The KEYNOTE-811 trial of dual PD-1 and HER2 blockade in HER2-positive gastric cancer, Nature 600 (7890) (2021) 727–730.
[5] K. Li, A. Zhang, X. Li, et al., Advances in clinical immunotherapy for gastric cancer, Biochim. Biophys. Acta Rev. Canc 1876 (2) (2021) 188615.
[6] C. Chen, F. Zhang, N. Zhou, et al., Efficacy and safety of immune checkpoint inhibitors in advanced gastric or gastroesophageal junction cancer: a systematic review and meta-analysis, OncoImmunology 8 (5) (2019) e1581547.
[7] I. Barbieri, T. Kouzarides, Role of RNA modifications in cancer, Nat. Rev. Cancer 20 (6) (2020) 303–322.
[8] Q. Wang, C. Chen, Q. Ding, et al., METTL3-mediated m(6)A modification of HDGF mRNA promotes gastric cancer progression and has prognostic significance, Gut 69 (7) (2020) 1193–1205.
[9] C. Zhang, M. Zhang, S. Ge, et al., Reduced m6A modification predicts malignant phenotypes and augmented Wnt/PI3K-Akt signaling in gastric cancer, Cancer Med. 8 (10) (2019) 4766–4781.
[10] Z. Chen, M. Qi, B. Shen, et al., Transfer RNA demethylase ALKBH3 promotes cancer progression via induction of tRNA-derived small RNAs, Nucleic Acids Res. 47 (5) (2019) 2533–2545.
[11] Y. Wang, J. Wang, X. Li, et al., N(1)-methyladenosine methylation in tRNA drives liver tumourigenesis by regulating cholesterol metabolism, Nat. Commun. 12 (1) (2021) 6314.
[12] X. Chen, A. Li, B.F. Sun, et al., 5-methylcytosine promotes pathogenesis of bladder cancer through stabilizing mRNAs, Nat. Cell Biol. 21 (8) (2019) 978–990.
[13] R. Yang, X. Liang, H. Wang, et al., The RNA methyltransferase NSUN6 suppresses pancreatic cancer development by regulating cell proliferation, EBioMedicine 63 (2021) 103195.
[14] L. Mei, C. Shen, R. Miao, et al., RNA methyltransferase NSUN2 promotes gastric cancer cell proliferation by repressing p57(Kip2) by an m(5)C-dependent manner, Cell Death Dis. 11 (4) (2020) 270.
[15] J. Ma, H. Han, Y. Huang, et al., METTL1/WDR4-mediated m(7)G tRNA modifications and m(7)G codon usage promote mRNA translation and lung cancer progression, Mol. Ther. 29 (12) (2021) 3422–3435.
[16] Z. Dai, H. Liu, J. Liao, et al., N(7)-Methylguanosine tRNA modification enhances oncogenic mRNA translation and promotes intrahepatic cholangiocarcinoma progression, Mol Cell 81 (16) (2021) 3339–3355 e3338.
[17] Z. Chen, W. Zhu, S. Zhu, et al., METTL1 promotes hepatocarcinogenesis via m(7) G tRNA modification-dependent translation control, Clin. Transl. Med. 11 (12) (2021) e661.

[18] E.A. Orellana, Q. Liu, E. Yankova, et al., METTL1-mediated m(7)G modification of Arg-TCT tRNA drives oncogenic transformation, Mol Cell 81 (16) (2021) 3323–3338 e3314.
[19] S. Jana, A.C. Hsieh, R. Gupta, Reciprocal amplification of caspase-3 activity by nuclear export of a putative human RNA-modifying protein, PUS10 during TRAIL-induced apoptosis, Cell Death Dis. 8 (10) (2017) e3093.
[20] D. Ruggero, S. Grisendi, F. Piazza, et al., Dyskeratosis congenita and cancer in mice deficient in ribosomal RNA modification, Science 299 (5604) (2003) 259–262.
[21] L. Montanaro, M. Calienni, S. Bertoni, et al., Novel dyskerin-mediated mechanism of p53 inactivation through defective mRNA translation, Cancer Res. 70 (11) (2010) 4767–4777.
[22] S. Delaunay, F. Rapino, L. Tharun, et al., Elp3 links tRNA modification to IRES-dependent translation of LEF1 to sustain metastasis in breast cancer, J. Exp. Med. 213 (11) (2016) 2503–2523.
[23] J. Chen, Y. Dang, W. Feng, et al., SOX18 promotes gastric cancer metastasis through transactivating MCAM and CCL7, Oncogene 39 (33) (2020) 5536–5552.
[24] Z.R. Chalmers, C.F. Connelly, D. Fabrizio, et al., Analysis of 100,000 human cancer genomes reveals the landscape of tumor mutational burden, Genome Med. 9 (1) (2017) 34.
[25] K.G. Yeoh, P. Tan, Mapping the genomic diaspora of gastric cancer, Nat. Rev. Cancer 22 (2) (2022) 71–84.
[26] D.C. Lazar, M.F. Avram, I. Romosan, et al., Prognostic significance of tumor immune microenvironment and immunotherapy: novel insights and future perspectives in gastric cancer, World J. Gastroenterol. 24 (32) (2018) 3583–3616.
[27] Y. Yu, X. Ma, Y. Zhang, et al., Changes in expression of multiple checkpoint molecules and infiltration of tumor immune cells after neoadjuvant chemotherapy in gastric cancer, J. Cancer 10 (12) (2019) 2754–2763.
[28] T.F. Gajewski, H. Schreiber, Y.X. Fu, Innate and adaptive immune cells in the tumor microenvironment, Nat. Immunol. 14 (10) (2013) 1014–1022.
[29] K. Yamashita, M. Iwatsuki, K. Harada, et al., Prognostic impacts of the combined positive score and the tumor proportion score for programmed death ligand-1 expression by double immunohistochemical staining in patients with advanced gastric cancer, Gastric Cancer 23 (1) (2020) 95–104.
[30] Z.A. Wainberg, C.S. Fuchs, J. Tabernero, et al., Efficacy of pembrolizumab monotherapy for advanced gastric/gastroesophageal junction cancer with programmed death ligand 1 combined positive score >/=10, Clin. Cancer Res. 27 (7) (2021) 1923–1931.
[31] K. Shitara, M. Ozguroglu, Y.J. Bang, et al., Pembrolizumab versus paclitaxel for previously treated, advanced gastric or gastro-oesophageal junction cancer (KEYNOTE-061): a randomised, open-label, controlled, phase 3 trial, Lancet 392 (10142) (2018) 123–133.
[32] F. Wang, X.L. Wei, F.H. Wang, et al., Safety, efficacy and tumor mutational burden as a biomarker of overall survival benefit in chemo-refractory gastric cancer treated with toripalimab, a PD-1 antibody in phase Ib/II clinical trial NCT02915432, Ann. Oncol. 30 (9) (2019) 1479–1486.
[33] S. Aviles-Vazquez, A. Chavez-Gonzalez, A. Hidalgo-Miranda, et al., Global gene expression profiles of hematopoietic stem and progenitor cells from patients with chronic myeloid leukemia: the effect of in vitro culture with or without imatinib, Cancer Med. 6 (12) (2017) 2942–2956.
[34] L. Darda, F. Hakami, R. Morgan, et al., The role of HOXB9 and miR-196a in head and neck squamous cell carcinoma, PLoS One 10 (4) (2015) e0122285.
[35] G. Sultan, S. Zubair, I.A. Tayubi, et al., Towards the early detection of ductal carcinoma (a common type of breast cancer) using biomarkers linked to the PPAR (gamma) signaling pathway, Bioinformation 15 (11) (2019) 799–805.
[36] H. Lee, B.C. Park, Kang J. Soon, et al., MAM domain containing 2 is a potential breast cancer biomarker that exhibits tumour-suppressive activity, Cell Prolif. 53 (9) (2020) e12883.